Microarray Analysis of Murine Retinal Light Damage Reveals Changes in Iron Regulatory, Complement, and Antioxidant Genes in the Neurosensory Retina and Isolated RPE

Majda Hadziahmetovic,[1] *Usha Kumar,*[2] *Ying Song,*[1] *Steven Grieco,*[1] *Delu Song,*[1] *Yafeng Li,*[1] *John W. Tobias,*[3] *and Joshua L. Dunaief*[1]

Purpose. The purpose of this study was to investigate light damage–induced transcript changes within neurosensory retina (NSR) and isolated retinal pigment epithelium (RPE). Similar studies have been conducted previously, but were usually limited to the NSR and only a portion of the transcriptome. Herein most of the transcriptome, not just in the NSR but also in isolated RPE, was queried.

Methods. Mice were exposed to 10,000 lux cool white fluorescent light for 18 hours and euthanized 4 hours after photic injury. NSR and isolated RPE were collected, and RNA was isolated. DNA microarray hybridization was conducted as described in the Affymetrix GeneChip Expression Analysis Technical Manual. Microarray analysis was performed using probe intensity data derived from the Mouse Gene 1.0 ST Array. For the genes of interest, confirmation of gene expression was done using quantitative real-time PCR. Immunofluorescence assessed protein levels and localization.

Results. Numerous iron regulatory genes were significantly changed in the light-exposed NSR and RPE. Several of these gene expression changes favored an iron-overloaded state. For example, the transferrin receptor was upregulated in both light-exposed NSR and RPE. Consistent with this, there was stronger transferrin receptor immunoreactivity in the light-exposed retinas. Significant changes in gene expression following light damage were also observed in oxidative stress and complement system genes.

Conclusions. The concept of a photooxidative stress–induced vicious cycle of increased iron uptake leading to further oxidative stress was introduced. (*Invest Ophthalmol Vis Sci.* 2012;53:5231–5241) DOI:10.1167/iovs.12-10204

From the [1]F.M. Kirby Center for Molecular Ophthalmology, Scheie Eye Institute, Perelman School of Medicine, University of Pennsylvania, Philadelphia, Pennsylvania; [2]Drexel University College of Medicine, Philadelphia, Pennsylvania; and [3]Penn Molecular Profiling Facility, Perelman School of Medicine, University of Pennsylvania, Philadelphia, Pennsylvania.

Supported by National Eye Institute/National Institutes of Health Grant EY015240, Research to Prevent Blindness (New York, NY), the F.M. Kirby Foundation, the Arnold and Mabel Beckman Initiative for Macular Research, and the Paul and Evanina Bell Mackall Foundation Trust.

Submitted for publication May 16, 2012; revised June 15, 2012; accepted June 21, 2012.

Disclosure: **M. Hadziahmetovic**, None; **U. Kumar**, None; **Y. Song**, None; **S. Grieco**, None; **D. Song**, None; **Y. Li**, None; **J.W. Tobias**, None; **J.L. Dunaief**, None

Corresponding author: Joshua L. Dunaief, 305 Stellar Chance Labs, 422 Curie Boulevard, Philadelphia, PA 19104; jdunaief@upenn.edu.

Iron is an essential metabolic component, but also a potent generator of damaging free radicals that can cause oxidative stress via the Fenton reaction. Regulation of ferrous iron levels is critical for meeting physiologic demand while preventing the toxicity associated with iron overload. Excess iron is toxic to different tissues including the retina. Homeostatic mechanisms for iron import, storage, and export are in place to regulate iron levels in the retina. Impairment of these mechanisms and resulting excess iron have been associated with retinal degeneration in aceruloplasminemia, Friedreich's ataxia, and pantothenate kinase–associated neurodegeneration.[1–5] Retinal iron dysregulation also leads to degeneration in mouse models.[6–10]

Acute light-induced retinal damage is a well-established retinal degeneration model. Since both light exposure and iron can induce retinal oxidative stress, it is plausible that these two agents synergistically promote retinal degeneration. Supporting this, iron chelation can ameliorate retinal light damage.[11,12]

In recent years several studies have demonstrated significant changes in retinal expression of iron handling genes following light exposure.[13–16] These studies primarily assessed the response of the neurosensory retina (NSR) to photooxidative damage. Now, with the advent of microarrays representing most of the transcriptome and techniques to obtain RNA from the isolated retinal pigment epithelium (RPE) monolayer, we have probed the response of the RPE and NSR to light damage. Surprisingly, the transferrin receptor, which could increase intracellular iron levels, creating a vicious cycle of oxidative stress, was upregulated. Changes in other iron regulatory, antioxidant, and complement genes were also of interest.

Materials and Methods

Animals

Male, 10-week-old Balb/cJ mice ($n = 8$) were obtained from a commercial laboratory (The Jackson Laboratory, Bar Harbor, ME). All procedures were approved by the Institutional Animal Care and Use Committee of the University of Pennsylvania and complied with the ARVO Statement for the Use of Animals in Ophthalmic and Vision Research.

Photic Injury

Mice ($n = 4$) were exposed to 10,000 lux cool white fluorescent light for 18 hours, as described previously,[14,15] with slight modifications. The control group ($n = 4$) was kept on a regular 12-hour light/dark cycle. Mice were euthanized 4 hours after photic injury ended, and the

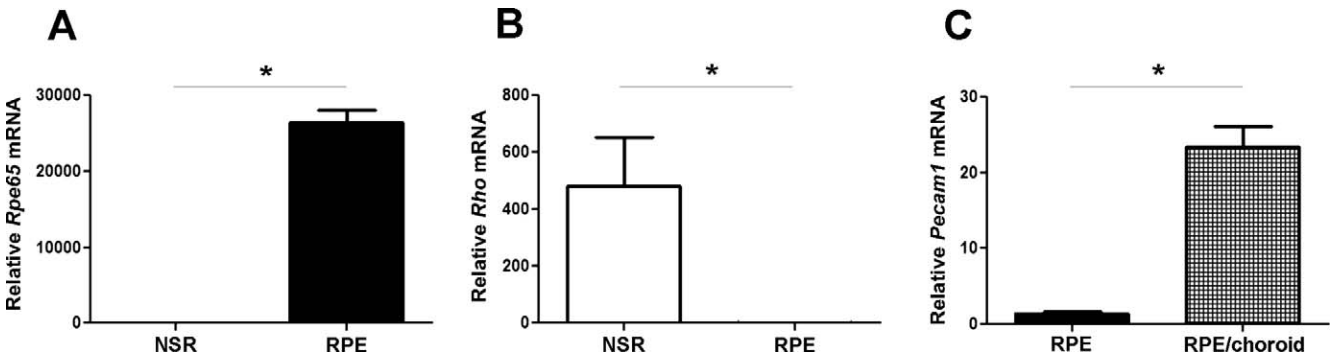

Figure 1. Purity of NSR and isolated RPE. Graphs showing *Rpe65* (**A**) *Rho* (**B**) mRNA levels within NSR and RPE and *Pecam1* (**C**) within RPE and RPE/choroid. Isolated RPE has significantly higher expression of *Rpe65* relative to NSR (NSR was normalized to 1), whereas NSR has significantly higher expression of *Rho* (RPE was normalized to 1). *Pecam1* mRNA is significantly higher within the RPE/choroid relative to RPE. $^*P < 0.05$.

NSR and isolated RPE were collected for mRNA quantification. Four samples per group were analyzed separately.

Neurosensory Retina and RPE Isolation

Purified RPE cells were isolated by removing the anterior segment (cornea, iris, and lens) from enucleated mouse eyes after a two-step digestion. The eyes were incubated at 37°C for 40 minutes in 2% w/v dispase in 1× Hanks' balanced salt solution (HBSS) with Ca^{2+} and Mg^{2+} (HBSS+) (Invitrogen, Carlsbad, CA). After digestion with dispase, slits were made in the cornea with a scalpel blade and the eyes were incubated for additional 10 minutes in 1 mg/mL hyaluronidase in HBSS without Ca^{2+} and Mg^{2+} (HBSS–). After two washes in HBSS+, the anterior segment was removed and the eyecup was placed in HBSS–, where the NSR was removed. The NSR was frozen on dry ice and stored at –80°C until the RNA isolation was performed (RNeasy Mini Kit; Qiagen Inc., Valencia, CA) according to the manufacturer's protocol. The RPE cells were gently brushed from the eyecup in fresh HBSS–, collected, and pelleted at 1200*g* for 15 minutes. The supernatant was removed and the cells were stored at –80°C until the RNA isolation was performed (RNeasy Micro Kit; Qiagen Inc.) according to the manufacturer's protocol. The purity of the NSR and isolated RPE cells was verified by relative quantification of RPE-specific 65-kDa protein (Rpe65) mRNA, specific to the RPE; rhodopsin (*Rho*), specific to the NSR; and platelet/endothelial cell adhesion molecule 1 (*Pecam1*), specific to vasculature.

DNA Microarray Hybridization

Microarray services were provided by the Penn Molecular Profiling Facility, including quality control tests of the total RNA samples (Agilent 2100 Bioanalyzer; Agilent Technologies, Santa Clara, CA; NanoDrop Spectrophotometer; NanoDrop Products, Wilmington, DE). All protocols were conducted as described in commercially available user guides and technical manuals (NuGEN Ovation User Guide; NuGEN Technologies, Inc., San Carlos, CA; and the Affymetrix GeneChip Expression Analysis Technical Manual; Affymetrix Inc., Santa Clara, CA). Briefly, 10 ng of total RNA was converted to first-strand cDNA using reverse transcriptase primed by poly(T) and random oligomers that incorporated an RNA priming region. Second-strand cDNA synthesis was followed by ribo-SPIA linear amplification of each transcript using an isothermal reaction with RNase, RNA primer, and DNA polymerase (Ovation Pico WTA System; NuGEN Technologies), and the resulting cDNA was fragmented, assessed by quality control testing (Bioanalyzer; Agilent Technologies), and biotinylated by terminal transferase end labeling. Labeled cDNA (3 μg) was added to hybridization cocktails (Affymetrix Inc.), heated at 99°C for 5 minutes, and hybridized for 16 hours at 45°C (to Mouse Gene 1 GeneChips; Affymetrix Inc.). The microarrays were then washed at low (6× SSPE) and high (100 mM MES, 0.1 M NaCl) stringency and stained with streptavidin-phycoerythrin. Fluorescence was amplified by adding biotinylated antistreptavidin and an additional aliquot of streptavidin-phycoerythrin stain. A confocal scanner was used to collect the fluorescence signal after excitation at 570 nm.

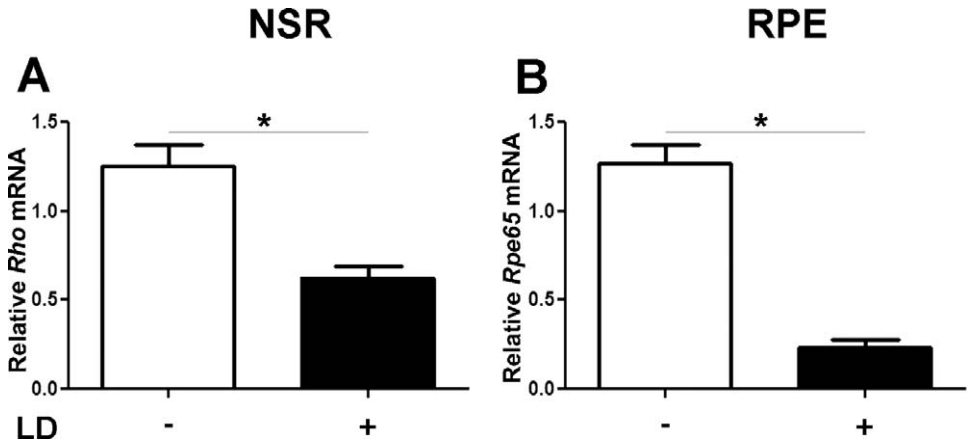

Figure 2. Light-induced changes in visual cycle genes. Graphs showing significant reduction in expression of *Rho* within NSR (**A**) and *Rpe65* within RPE (**B**) following light damage, measured by qPCR. $^*P < 0.05$.

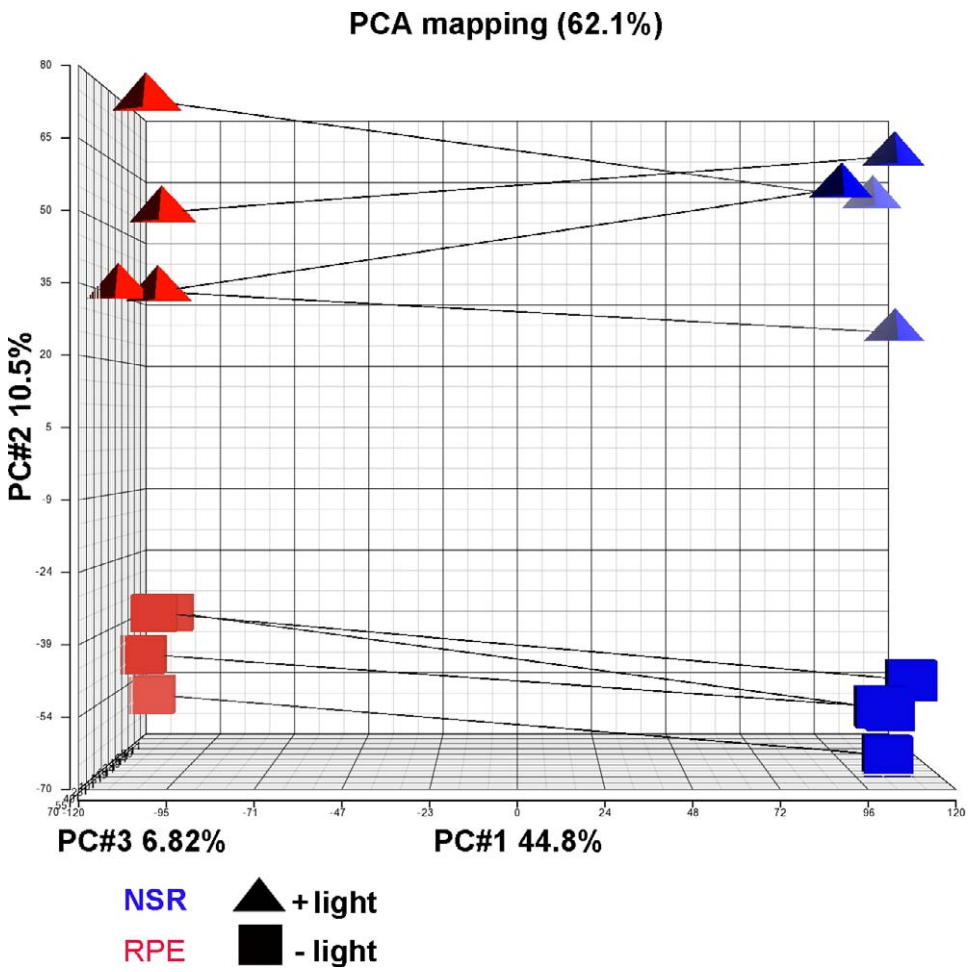

Figure 3. PCA of the processed microarray gene expression data. PCA analysis using all genes where NSR is represented in *blue* and RPE in *red*, and light exposure and no light exposure as *triangles* and *squares*, respectively. Tissue type (NSR and RPE) is the strongest determinant of global gene expression variability and is captured by the first principal component (*x*-axis). Light exposure is captured by the second principal component (*y*-axis).

Data Analysis

Microarray analysis was performed using probe intensity data (.cel files; derived from the Mouse Gene 1.0 ST Array; Affymetrix Inc.). The microarray data were analyzed using commercial software (Partek Genomics Suite, version 6.6; Partek Inc., St. Louis, MO). CEL files (Affymetrix Inc.) were imported into the commercial software suite (Partek Inc.) and background correction, normalization, and summa-

Table 1. List of Differentially Expressed Iron Regulatory Genes in Neurosensory Retina following Light Damage

Gene Title, Gene Symbol	Fold Change	Step-up (*P* Value)	Affymetrix Transcript Cluster ID
Heme oxygenase (decycling) 1, *Hmox1*	6.70	0.002	10572897
Lipocalin 2, *Lcn2*	4.35	0.002	10481627
Ceruloplasmin, *Cp*	3.87	0.02	10490989
Solute carrier family 25, member 37, *Slc25a37*	3.48	0.001	10421172
Transferrin, *Trf*	3.24	0.0003	10596148
Cytochrome b-245, beta polypeptide, *Cybb*	2.73	0.01	10603551
Radical S-adenosyl methionine domain containing 2, *Rsad2*	2.59	0.01	10399710
STEAP family member 4, *Steap4*	2.29	0.02	10519497
Cytochrome p450, family 1, subfamily b, polypeptide 1, *Cyp1b1*	1.97	0.002	10453057
Ferritin light chain 1, *Ftl1*	1.89	0.0007	10447591
Cholesterol 25-hydroxylase, *Ch25h*	1.87	0.03	10467136
Ferritin light chain 2, *Ftl2*	1.77	0.001	10406198
Aldehyde oxidase 1, *Aox1*	1.61	0.01	10346374
Sideroflexin 5, *Sfxn5*	−1.58	0.07	10545812
Hemochromatosis, *Hfe*	−1.79	0.003	10408227
Protein phosphatase, EF-hand calcium binding domain 2, *Ppef2*	−2.09	0.006	10531348

TABLE 2. List of Differentially Expressed Iron Regulatory Genes in Retinal Pigment Epithelium following Light Damage

Gene Title, Gene Symbol	Fold Change	Step-up (*P* Value)	Affymetrix Transcript Cluster ID
Lipocalin 2, *Lcn2*	23.71	0.0006	10481627
Heme oxygenase (decycling) 1, *Hmox1*	4.84	0.002	10572897
Transferrin receptor, *Tfrc*	2.45	0.0009	10435075
STEAP family member 4, *Steap4*	2.14	0.02	10519497
Cytochrome P450, family 20, subfamily A, polypeptide 1, *Cyp20a1*	1.79	0.02	10346747
Cholesterol 25-hydroxylase, *Ch25h*	1.63	0.04	10467136
ATP-binding cassette, subfamily E (OABP) member 1, *Abce1*	1.60	0.002	10579874
Ferredoxin 1-like, *Fdx1l*	1.57	0.007	10591423
Leprecan 1, *Lepre1*	1.54	0.003	10507612
Superoxide dismutase 2, mitochondrial, *Sod2*	1.52	0.002	10441815
Cytochrome P450, family 27, subfamily a, polypeptide 1, *Cyp27a1*	−1.51	0.02	10347481
Apoptosis-inducing factor, mitochondrion-associated 3, *Aifm3*	−1.52	0.02	10434007
Prostaglandin I2 (prostacyclin) synthase, *Ptgis*	−1.55	0.01	10489878
Stearoyl-Coenzyme A desaturase 2, *Scd2*	−1.59	0.009	10463355
Sterol-C4-methyl oxidase-like, *Sc4mol*	−1.78	0.006	10578916
Hephaestin, *Heph*	−1.81	0.01	10600857
Cytochrome P450 family 51, *Cyp51*	−1.81	0.008	10527920
Protein phosphatase, EF-hand calcium binding domain 2, *Ppef2*	−2.08	0.004	10531348
Dihydropyrimidine dehydrogenase, *Dpyd*	−2.16	0.01	10495625
Bone morphogenetic protein 6, *Bmp6*	−2.26	0.003	10404686

rization were applied using the robust multiarray average (RMA) yielding log 2 transformed intensities for the approximately 28,000 transcripts covered by the array. Global variation among the experimental samples was evaluated with principal components analysis (PCA). A two-way ANOVA was performed with factors for tissue (RPE, NSR) and light (+/−), with an additional term for the interaction of tissue and light. The two pairwise contrasts for light exposure within each tissue were calculated as well, each yielding a *P* value and fold change for each gene. The three *P* values from the ANOVA and the two from the contrasts were adjusted for false discovery rate (FDR) by the step-up method of Benjamini and Hochberg as encoded in the commercial software suite (Partek Inc.).

Genes on the array were scored for participation in three particular areas of interest using the bioinformatics initiative, Gene Ontology (GO, http://geneontology.org) annotations. Lists downloaded from GO of mouse gene symbols having terms related to "iron," "oxidative stress," and "complement" were merged with the array annotations. In all, 373 genes were scored as associated with "iron," 77 with "oxidative stress," and 44 with "complement."

In parallel, the NSR and RPE differentially expressed gene (DEG) lists were then created by filtering for step-up value of $P < 0.05$ (NSR+ vs. NSR− or RPE+ vs. RPE−) and fold-change $> \pm 1.5$. There were 813 genes on the NSR DEG list and 1180 on the RPE list.

Sorting by fold change, lists of the top ten most up- and downregulated genes for NSR+/− and RPE+/− were generated. Further, the RPE and the NSR DEG lists were evaluated for genes known to be related to retinal disease (eyeGENE; National Ophthalmic Disease Genotyping and Phenotyping Network, National Eye Institute/National Institutes of Health, Bethesda, MD).

Quantitative Real-Time PCR (qPCR)

Gene expression from the neurosensory retina and RPE samples used for microarray analysis was additionally analyzed using quantitative real-time PCR as previously published.[10] Gene expression assays were obtained (*Taq*Man; Applied Biosystems, Foster City, CA) and used for PCR analysis. Probes used were rhodopsin (*Rho*, Mm00520345_m1), (*Rpe65*, Mm00504133_m1), (*Pecam1*, Mm01242584_m1), heme oxygenase (decycling) 1 (*Hmox1*, Mm00516005_m1), catalase (*Cas-1*, Mm00437992_m1), glutathione peroxidase 1 (*Gpx*, Mm00656767_g1), superoxide dismutase 1 (*Sod1*, 01700393_g1), complement component 3 (*C3*, Mm00486101_m1), complement component 3a receptor 1 (*C3ar1*, Mm02620006_s1), Cd59b antigen (*Cd59b*, Mm02525679_s1), transferrin receptor (*Tfrc*, Mm00441941_m1), hephaestin (*Heph*, Mm00515970_m1), ferritin light chain-L1 (*Ftl1*, Mm03030144_g1). Eukaryotic 18S rRNA (Hs99999901_s1) served as an internal control. Real-time RT-PCR (*Taq*Man; Applied Biosystems) was performed on a commercial sequence detection system (ABI Prism 7500; Applied Biosystems) using the $\Delta\Delta C_T$method. All reactions were performed in biological quadruplicates (four mice) and technical triplicates (three real-time PCR replicates per mouse).

Statistical Analysis for qPCR

The mean of four samples and the SE were calculated for each comparison group. The means between the groups were compared using the two-group *t*-test. A value of $P < 0.05$ was considered to be statistically significant. Correction for multiple comparisons was not performed. Data are reported as means ± SEM. All statistical analysis was performed with a commercial software package (GraphPad Prism version 5; GraphPad Software, San Diego, CA).

Immunofluorescence

The immunofluorescence was performed as previously published[17] on an additional set of samples. Briefly, mouse globes were fixed in 4% paraformaldehyde for 10 minutes, followed by infiltration in 30% sucrose overnight. Then the eyecups were embedded in optimal cutting temperature compound (Tissue-Tek; Sakura Finetek, Torrance, CA). Immunofluorescence was performed on sections 10 μm thick. Primary antibody used was rat anti-transferrin receptor-1 at 1–100 (AbD Serotec, Düsseldorf, Germany) and mouse anti-CD31 (PECAM1) AT 1–100 (BD Biosciences, San Jose, CA). Primary antibody reactivity was detected using Cy3 fluorophore conjugated secondary antibodies (Jackson ImmunoResearch Laboratories, West Grove, PA). Control sections were treated identically, except that primary antibody was omitted. Sections were analyzed by fluorescence microscopy with identical exposure parameters (Nikon TE300 microscope [Nikon, Tokyo, Japan], with ImagePro Plus version 6.1 software; Media Cybernetics Inc., Bethesda, MD). Quantification of immunoreactivity was performed by measuring the mean pixel intensity within the RPE and neurosensory retina of each photomicrograph.

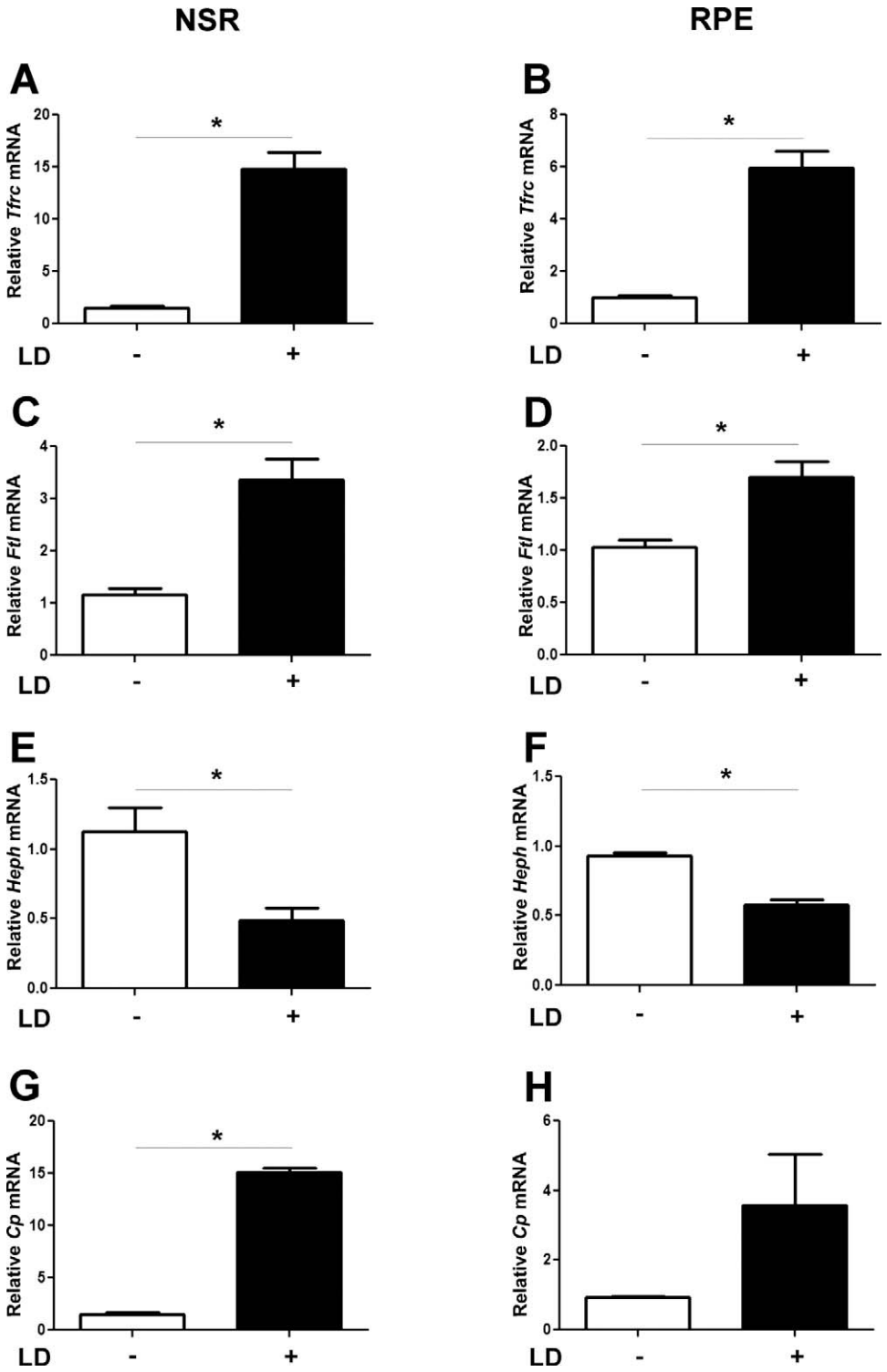

Figure 4. Light-induced changes in iron regulatory genes expression measured by qPCR. Graphs showing significant changes in mRNA levels for iron regulatory genes in NSR following light damage (LD) (**A**, **C**, **E**, **G**). The *right column* shows changes of the same genes within the isolated RPE (**B**, **D**, **F**, **H**). $^*P < 0.05$.

Results

Purity of the Isolated NSR and RPE

The purity of control NSR and isolated RPE was verified by relative quantification of mRNAs specific for retinal pigment epithelium (*Rpe65*), photoreceptors (*Rho*), and abundant in vascular endothelial cells (*Pecam1*). The *Rpe65* mRNA levels were compared between NSR and RPE by qPCR and found to be almost 30,000-fold higher in the isolated RPE cells (Fig. 1A), indicating minimal NSR contamination with RPE cells. Similarly, *Rho* was 400-fold higher within the NSR relative to RPE (Fig. 1B), additionally verifying purity of the isolated RPE. To assess RPE contamination with choroid, we compared *Pecam1* mRNA

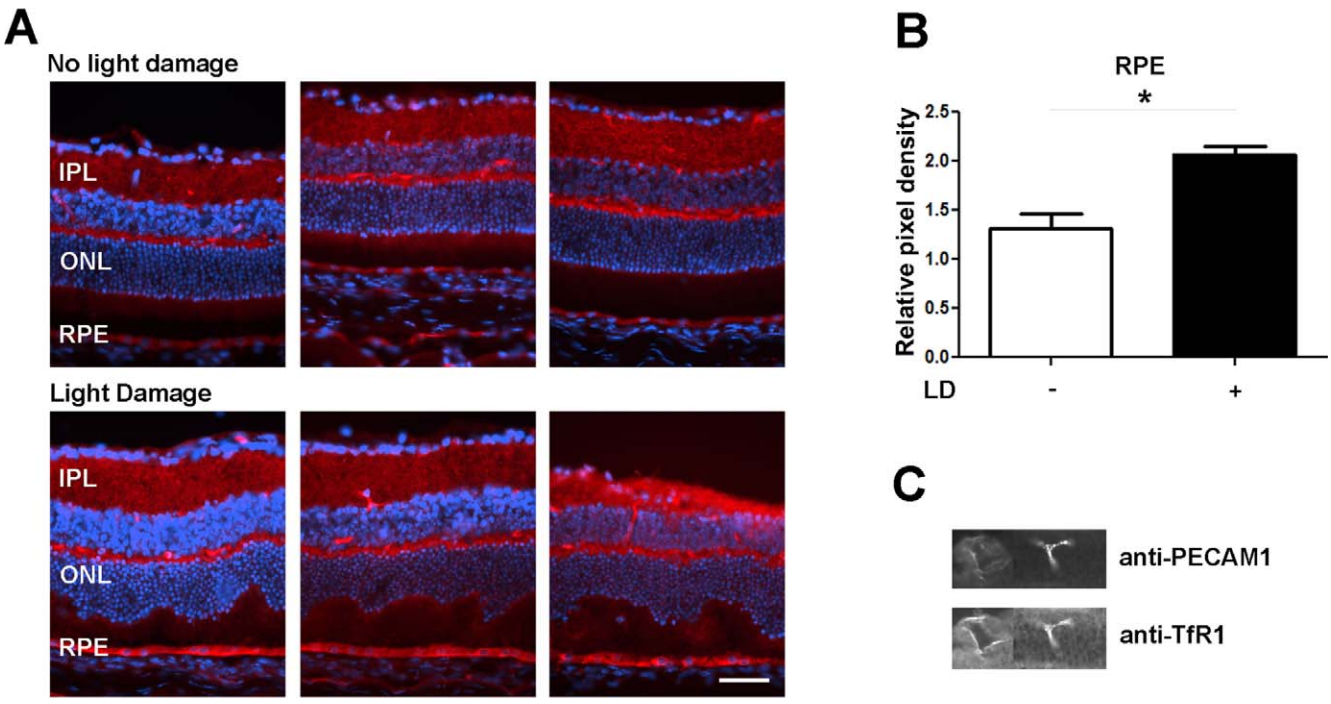

Figure 5. Light damaged retinas have increased TfR1 immunoreactivity. Fluorescence photomicrographs of light-damaged retinas ($n = 3$; **A**, *bottom panels*) show increase in TfR1 immunoreactivity relative to untreated controls ($n = 3$ each, *top panels*; scale bar: 25 μm). Relative pixel density for TfR1 within the RPE (**B**) shows significantly higher immunoreactivity in LD samples relative to untreated. Double-labeling of PECAM-1 (**C**, *top*) and TfR1 (**C**, *bottom*) shows colocalization with endothelial cells. $^*P < 0.05$.

levels between isolated RPE and RPE/choroid. The choroid expresses this gene due to the presence of vasculature. *Pecam1* mRNA levels were 20-fold higher in RPE/choroid (Fig. 1C) than in isolated RPE, indicating only slight contamination of the isolated RPE cells with choroid.

Photic Injury and Retinal Damage

To confirm that exposure to light caused retinal damage we performed qPCR for *Rho* and *Rpe65*. Light exposure caused significant reduction in *Rho* expression within NSR, suggesting severe photoreceptor damage (Fig. 2A). Analogously in the RPE, *Rpe65* was significantly reduced following photic injury (Fig. 2B). Previously we have reported retinal morphology following the light damage.[15] Our protocol causes severe retinal degeneration with thinning of the outer nuclear layer and disruption of inner and outer segments by 10 days after light exposure.

Global Perspective of Microarray Results

In response to light damage, in the NSR 595 genes were upregulated and 218 were downregulated. In contrast, in the RPE more genes (611) were downregulated than upregulated (569). PCA reveals close correspondence in global gene expression levels in the no light group, and a wide separation from the light-exposed group (Fig. 3). Among the four light-exposed mice, there was moderate separation, most likely reflecting biological variability in light damage severity and/or response to light. The full set of microarray data has been deposited in the National Center for Biotechnology Information Gene Expression Omnibus repository under accession number GSE37773. Because iron dysregulation, oxidative stress, and complement have been implicated in light damage and human retinal degenerations, the following sections will describe light-induced changes in genes from these categories. Although genes assigned to these categories as a group did not show statistically significant changes by the Fisher exact test, a number of genes in each category were significantly altered.

Light Damage and Iron Homeostasis

Microarray analysis showed that photic injury causes significant changes in several retinal iron regulatory genes, seemingly favoring increased iron uptake (Tables 1 and 2). Since microarray is not as quantitative as qPCR, we confirmed gene expression changes by qPCR. In addition, since qPCR is more sensitive than microarray, we used qPCR to test some iron regulatory genes that did not show expression changes in the microarray analysis. We confirmed by qPCR significant

Table 3. List of Differentially Expressed Oxidative Stress Genes in Neurosensory Retina following Light Damage

Gene Title, Gene Symbol	Fold Change	Step-up (*P* Value)	Affymetrix Transcript Cluster ID
Heme oxygenase (decycling) 1, *Hmox1*	6.71	0.002	10572897
Growth factor receptor bound protein 2-associated protein 1, *Gab1*	1.65	0.006	10579925
Uveal autoantigen with coiled-coil domains and ankyrin repeats, *Uaca*	1.51	0.01	10586017
Apolipoprotein E, *Apoe*	–1.75	0.004	10560624

Table 4. List of Differentially Expressed Oxidative Stress Genes in Retinal Pigment Epithelium following Light Damage

Gene Title, Gene Symbol	Fold Change	Step-up (*P* Value)	Affymetrix Transcript Cluster ID
Glutamate-cysteine ligase, catalytic subunit, *Gclc*	1.89	0.02	10587266
Sulfiredoxin 1 homolog, *Srxn1*	1.63	0.02	10477061
Superoxide dismutase 2 mitochondrial, *Sod2*	1.52	0.002	10441815
Peroxiredoxin 6, *Prdx6*	–1.50	0.005	10359422
Nonmetastatic cells 5, protein expressed in (nucleoside-diphosphate kinase), *Nme5*	–2.55	0.02	10458122
NAD(P)H dehydrogenase quinone 1, *Nqo1*	–3.76	0.003	10581538

upregulation of transferrin receptor 1 mRNA within both NSR and isolated RPE (Figs. 4A, 4B), as well as ferritin light chain upregulation in both tissues (Figs. 4C, 4D). Transferrin receptor (TfR1) mediates cellular iron uptake, whereas ferritin is the major iron storage protein. Additionally, expression of the ferroxidase hephaestin went significantly down in both tissues following light damage (Figs. 4E, 4F), whereas its homolog ceruloplasmin's expression was significantly upregulated in NSR only (Figs. 4G, 4H). To localize TfR1, retinas from mice following light damage were compared with untreated controls using immunofluorescence with an anti-TfR1 antibody (Fig. 5A). TfR1 immunoreactivity was stronger throughout the whole retina following the photic injury relative to untreated controls. This effect was the most pronounced within the RPE, where relative pixel density showed a significant difference (Fig. 5B). TfR1 also colocalized with the marker for endothelial cells PECAM-1 (Fig. 5C).

Light Damage and Oxidative Stress

Microarray analysis performed on NSR and isolated RPE samples following light damage showed, as expected, marked elevation of several genes related to oxidative stress (Tables 3 and 4). To better quantify obtained results we performed qPCR for some of these genes. Within NSR light damage caused significant increases in heme oxygenase-1, catalase, glutathione peroxidase, and superoxide dismutase 1 expression (Figs. 6A, 6C, 6E, 6G). RPE samples showed significant elevation of heme oxygenase-1 and glutathione peroxidase following the insult (Figs. 6B, 6F), whereas catalase and superoxide dismutase 1 showed no change (Figs. 6D, 6H).

Light Damage and Complement

Following light damage, microarray analysis also showed significant elevation of genes related to the complement system (Tables 5 and 6). Additional confirmation of these results by qPCR showed that following light damage *C3* and *C3ra1* were significantly upregulated within NSR (Figs. 7A, 7C). *C3* was also significantly upregulated within the isolated RPE (Fig. 7B), whereas within the isolated RPE protectin (*Cd59b*) a complement regulatory protein that inhibits the membrane attack complex (MAC) was significantly downregulated (Fig. 7F). This change was not observed within NSR.

Differential Expression of Genes Related to Ophthalmic Diseases following Light Damage

We compared our microarray data to the database of genes and diseases currently being tested (eyeGENE; National Ophthalmic Disease Genotyping Network through the National Eye Institute [http://www.nei.nih.gov/resources/eyegene/tableforgenes.asp]). Following light damage, expression of 12 genes known to be related to six ophthalmic diseases were altered within the NSR (Table 7), whereas expression of 6 genes related to six ophthalmic diseases was changed within the isolated RPE (Table 8). Several of the genes, including complement factor 3, *ApoE*, and *TLR3* have been implicated in age-related macular degeneration (AMD), and two have been associated with Stargardt's disease: *ELOVL4* and *ABCA4*.

Discussion

Light-induced retinal degeneration has been studied in experimental animals for several decades. In the retina, absorption of light results in generation of reactive oxygen species (ROS). ROS have been shown to result in retinal cell damage and death. RPE cells and photoreceptors are particularly susceptible to oxidative damage due to high oxygen tension, large numbers of mitochondria, and abundant polyunsaturated fatty acids in photoreceptor membranes.[18] When photooxidative stress is severe, cells may respond to the insult by undergoing apoptosis. Additionally, iron overload can cause retinal degeneration and has been implicated in pathogenesis of AMD.[19] In our previous work we have shown that light damage caused elevation of retinal ceruloplasmin levels, in particular within the Müller cells.[14] This elevation of the ferroxidase ceruloplasmin may protect the retina against oxidative stress by decreasing the amount of ferrous iron available to produce ROS. In this study we use an updated, whole transcriptome microarray to further elucidate the role of light damage on alteration of gene expression within the retina, including genes that are responsible for tight regulation of retinal iron levels. One novelty of this study is that by using isolated RPE cells we can better understand the response of this cell type to light-induced retinal damage. Our results suggest that light-induced upregulation of transferrin receptor

Table 5. List of Differentially Expressed Complement System Genes in Neurosensory Retina following Light Damage

Gene Title, Gene Symbol	Fold Change	Step-up (*P* Value)	Affymetrix Transcript Cluster ID
Alpha-2-macroglobulin, *A2m*	6.49	0.0001	10541354
Complement component 3a receptor 1, *C3ar1*	4.39	0.005	10547657
Serine (or cysteine) peptidase inhibitor, clade G member 1, *Serping1*	3.97	0.005	10484463
Complement component factor i, *Cfi*	2.32	0.02	10496001
Complement component 3, *C3*	1.89	0.008	10452316

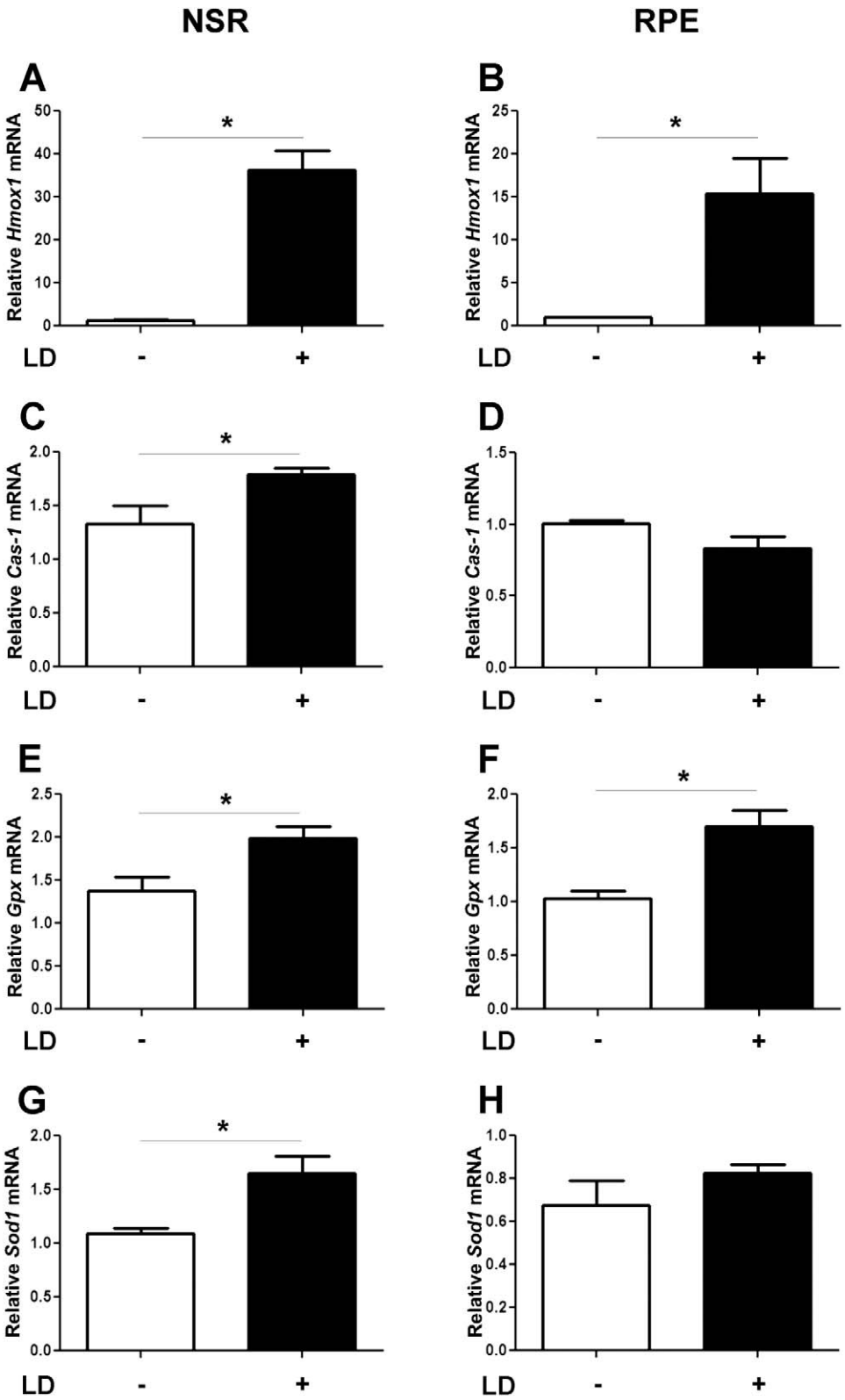

FIGURE 6. Light-induced changes in oxidative stress–related genes measured by qPCR. Graphs showing significant upregulation in *Hmox1*, *Cas-1*, *Gpx*, and *Sod1* mRNA levels in NSR following LD (**A**, **C**, **E**, **G**). The *right column* shows oxidative stress–related genes in RPE following LD, with only *Hmox1* and *Gpx* being significantly upregulated (**B**, **D**, **F**, **H**). $^*P < 0.05$.

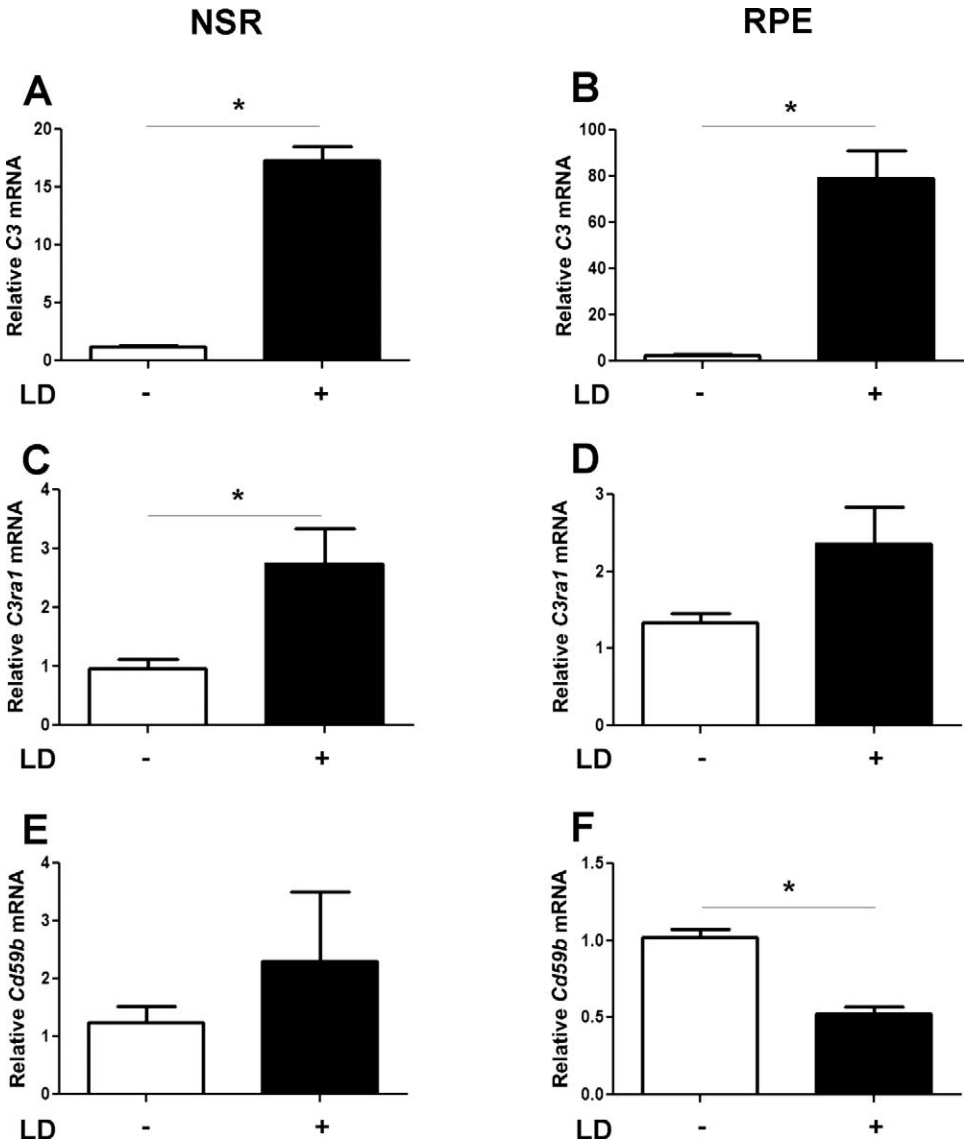

Figure 7. Light-induced changes in complement system–related genes measured by qPCR. Graphs showing significant upregulation of *C3*, *C3ra1* mRNA levels in NSR following LD (**A**, **C**, **E**). The *right column* shows complement system–related genes in RPE following LD (**B**, **D**, **F**). $^*P < 0.05$.

could lead to a vicious cycle of iron uptake and oxidative stress.

As expected, light damage caused significant changes in expression of several genes related to oxidative stress (Tables 3 and 4; Fig. 3). One of these genes, upregulated within both NSR and isolated RPE, is *Hmox1*. Under oxidative stress conditions, *Hmox1* can have a dual role: it may protect cells by inducing the catabolism of prooxidant heme and hemoproteins to the antioxidants, biliverdin and bilirubin, but *Hmox1* also catalyzes production of ferrous iron and carbon monoxide that may exacerbate cellular injury and oxidative stress by generating free radicals.[20–22] Broad upregulation of the genes associated with oxidative stress within the NSR, but not isolated RPE, suggests that this modification might be an attempt of the neural retina to protect itself from further damage. In contrast, following the light damage RPE cells did not upregulate catalase. This could make more hydrogen peroxide available to react with the iron taken up by the

Table 6. List of Differentially Expressed Complement System Genes in Retinal Pigment Epithelium following Light Damage

Gene Title, Gene Symbol	Fold Change	Step-up (*P* Value)	Affymetrix Transcript Cluster ID
Complement component 3, *C3*	2.52	0.002	10452316
Complement component 4B, *C4b*	2.41	0.01	10450242
Complement component factor i, *Cfi*	2.38	0.01	10496001
Alpha-2-macroglobulin, *A2m*	2.33	0.001	10541354
CD59b antigen, *Cd59b*	−2.11	0.005	10474223

Table 7. List of Differentially Expressed Genes Previously Related to Retinal Disease in Neurosensory Retina following Light Damage

Disease	Gene Title, Gene Symbol	Fold Change	Step-up (*P* Value)	Affymetrix Transcript Cluster ID
Glaucoma	Cytochrome P450, family 1, subfamily b, polypeptide 1, *Cyp1b1*	1.97	0.002	10453057
	Optineurin, *Optn*	–1.61	0.0007	10479833
AMD	Complement component 3, *C3*	1.89	0.008	10452316
	Toll-like receptor 3, *Tlr3*	1.78	0.01	10578493
	Apolipoprotein E, *Apoe*	–1.75	0.004	10560624
Sorsby Fundus Dystrophy, AMD	Tissue inhibitor of metalloproteinase 3, *TIMP3*	1.67	0.02	10365482
Retinitis Pigmentosa (RP) and Retinal Degenerations	PRP31 pre-mRNA processing factor 31 homolog (yeast), *Prpf31*	1.66	0.007	10549552
	Inosine 5′-phosphate dehydrogenase 1, *Impdh1*	–1.54	0.03	10543572
	Crumbs homolog 1 (Drosophila), *Crb1*	–2.14	0.003	10358283
	Nuclear receptor subfamily 2, group E, member 3, *Nr2e3*	–2.79	0.003	10594188
Cone rod dystrophy, Stargardt Disease, AMD, RP, and Retinal Degenerations	ATP-binding cassette, subfamily A (ABC1), member 4, *Abca4*	–1.63	0.004	10495712
Stargardt Disease	Elongation of very long chain fatty acids (FEN1/Elo2, SUR4/Elo3, yeast)-like 4, *Elovl4*	–1.53	0.03	10595392

upregulated transferrin receptor, in effect producing more of the highly reactive hydroxyl radical. Another seemingly maladaptive behavior of RPE was downregulation of Cd59b, a complement regulatory protein that inhibits the MAC. Reduction in genes that regulate or inhibit the complement system might be detrimental to the RPE. Similarly, reduction in one of the major membrane-associated complement regulatory proteins, CD46, has been reported in AMD.[23] Decreased expression of a complement regulatory gene combined with increased expression of C3 and the receptor for the C3 cleavage product C3a suggest that complement expression within the neural retina and RPE may contribute to the retinal degeneration induced by bright light. A previous light damage study found C3 and C3aR upregulation in macrophages and microglia in the neural retina.[24] Further, knockout of complement alternative pathway activator factor D diminishes retinal light damage.[25]

Maintaining iron homeostasis is critical for retinal health because excess iron may be toxic to the retina. Elevation of retinal iron levels is a normal part of aging, but also has been observed in retinal degenerations such as AMD and aceruloplasminemia. In this study we investigated whether light-induced oxidative stress within the NSR and isolated RPE is associated with changes in expression of iron homeostasis–related genes. We expected that following light damage, the retina would downregulate *Tfrc* to protect itself from further oxidative damage, but both NSR and RPE significantly upregulated *Tfrc* (Fig. 6). Tfrc mRNA stability is regulated by labile iron levels, with increased labile iron resulting in decreased Tfrc mRNA.[26,27] Our results suggest that despite severe oxidative stress the retina may incur further damage by importing more iron. Consistent with our mRNA data, TfR1 protein levels were elevated following the photic injury. We localized TfR1 immunoreactivity (Fig. 7) and observed strong RPE labeling, especially basally, suggesting choroidal vasculature as one of the sources of excess iron. Additionally, we colabeled with TfR1 and PECAM-1 and found that the retinal vasculature also has a strong TfR1 label. This finding suggests that the retinal vascular endothelial cells may use TfR1 for retinal iron transport. TfR1 upregulation has been reported in other (nonocular) cell types in response to oxidative stress, and most likely results from conversion by reactive oxygen species of iron regulatory protein 1 to its iron response element binding form.[28–30] This form stabilizes the Tfrc mRNA.[31]

Despite the fact that upon the light damage both NSR and RPE significantly upregulated *Tfrc*, only NSR counteracted this by significant upregulation of ceruloplasmin, a multicopper ferroxidase that facilitates iron export from the cell. Following the light damage, *Cp* homolog hephaestin was significantly downregulated in both tissues. These results suggest that Cp and Heph are regulated differently, perhaps to facilitate some distinct roles of each protein. Further, both *Hfe* and *Bmp6* were downregulated. Since these are most likely inhibitors of

Table 8. List of Differentially Expressed Genes Previously Related to Retinal Disease in Retinal Pigment Epithelium following Light Damage

Disease	Gene Title, Gene Symbol	Fold Change	Step-up (*P* Value)	Affymetrix Transcript Cluster ID
Age-related Macular Degeneration (AMD)	HtrA serine peptidase 1, *Hbtra1*	1.93	0.002	10558150
Doyne Honeycomb Dystrophy, AMD	Epidermal growth factor-containing fibulin-like extracellular matrix, protein 1, *Efemp1*	1.77	0.01	10374777
Sorsby Fundus Dystrophy, AMD	Tissue inhibitor of metalloproteinase 3, *TIMP3*	–1.57	0.01	10365482
Retinitis Pigmentosa (RP) and Retinal Degenerations	C1q and tumor necrosis factor related protein 5, *C1qtnf5*	–1.58	0.005	10584653
Cone rod dystrophy, Stargardt Disease, RP, and Retinal Degenerations	ATP-binding cassette, subfamily A (ABC1), member 4, *Abca4*	–1.66	0.003	10495712
Stargardt Disease	Elongation of very long chain fatty acids (FEN1/Elo2, SUR4/Elo3, yeast)-like 4, *Elovl4*	–1.72	0.03	10595392

retinal iron import,[9,32] their downregulation is predicted to result in increased retinal iron import.

Additionally, *Elovl4* and *Abcr* genes were significantly downregulated within the NSR and RPE following light damage. These genes associated with inherited macular degenerative diseases encode proteins that function in the processing of lipids in photoreceptor cells and were thought to be photoreceptor specific.[33,34] Interestingly we observed their expression within the RPE, as well as significant alterations following the photic injury. In no light damage, samples of *Elovl4* had a 6-fold higher expression within the NSR relative to RPE; *Abca4* was only 1.6-fold higher, suggesting its abundance within the RPE. Since the NSR relative to RPE showed 400-fold higher expression of *Rho* mRNA (Fig. 1B), contamination of RPE with photoreceptor mRNA is unlikely to explain the presence of these mRNAs in our isolated RPE cells. Thus, these genes may have important functions in the RPE.

Our data suggest that following photic injury, the retina alters expression of iron regulatory genes that favor increased iron uptake. Increased labile iron may cause additional oxidative stress in a vicious cycle of cellular self-destruction.

References

1. Egan RA, Weleber RG, Hogarth P, et al. Neuro-ophthalmologic and electroretinographic findings in pantothenate kinase-associated neurodegeneration (formerly Hallervorden-Spatz syndrome). *Am J Ophthalmol*. 2005;140:267–274.
2. Gitlin JD. Aceruloplasminemia. *Pediatr Res*. 1998;44:271–276.
3. Dunaief JL, Richa C, Franks EP, et al. Macular degeneration in a patient with aceruloplasminemia, a disease associated with retinal iron overload. *Ophthalmology*. 2005;112:1062–1065.
4. Noval S, Contreras I, Sanz-Gallego I, Manrique RK, Arpa J. Ophthalmic features of Friedreich ataxia. *Eye*. 2012;26:315–320.
5. Fortuna F, Barboni P, Liguori R, et al. Visual system involvement in patients with Friedreich's ataxia. *Brain*. 2009;132:116–123.
6. Hadziahmetovic M, Dentchev T, Song Y, et al. Ceruloplasmin/hephaestin knockout mice model morphologic and molecular features of AMD. *Invest Ophthalmol Vis Sci*. 2008;49:2728–2736.
7. Hahn P, Qian Y, Dentchev T, et al. Disruption of ceruloplasmin and hephaestin in mice causes retinal iron overload and retinal degeneration with features of age-related macular degeneration. *Proc Natl Acad Sci USA*. 2004;101:13850–13855.
8. Gnana-Prakasam JP, Tawfik A, Romej M, et al. Iron-mediated retinal degeneration in haemojuvelin-knockout mice. *Biochem J*. 2012;441:599–608.
9. Hadziahmetovic M, Song Y, Wolkow N, et al. Bmp6 regulates retinal iron homeostasis and has altered expression in age-related macular degeneration. *Am J Pathol*. 2011;179:335–348.
10. Hadziahmetovic M, Song Y, Ponnuru P, et al. Age-dependent retinal iron accumulation and degeneration in hepcidin knockout mice. *Invest Ophthalmol Vis Sci*. 2011;52:109–118.
11. Li ZL, Lam S, Tso MO. Desferrioxamine ameliorates retinal photic injury in albino rats. *Curr Eye Res*. 1991;10:133–144.
12. Song D, Song Y, Hadziahmetovic M, Zhong Y, Dunaief JL. Systemic administration of the iron chelator deferiprone protects against light-induced photoreceptor degeneration in the mouse retina. *Free Radic Biol Med*. 2012;53:64–71.
13. Picard E, Ranchon-Cole I, Jonet L, et al. Light-induced retinal degeneration correlates with changes in iron metabolism gene expression, ferritin level, and aging. *Invest Ophthalmol Vis Sci*. 2011;52:1261–1274.
14. Chen L, Dentchev T, Wong R, et al. Increased expression of ceruloplasmin in the retina following photic injury. *Mol Vis*. 2003;9:151–158.
15. Chen L, Wu W, Dentchev T, et al. Light damage induced changes in mouse retinal gene expression. *Exp Eye Res*. 2004;79:239–247.
16. Picard E, Fontaine I, Jonet L, et al. The protective role of transferrin in Muller glial cells after iron-induced toxicity. *Mol Vis*. 2008;14:928–941.
17. Dunaief JL, Dentchev T, Ying GS, Milam AH. The role of apoptosis in age-related macular degeneration. *Arch Ophthalmol*. 2002;120:1435–1442.
18. Zarbin MA. Current concepts in the pathogenesis of age-related macular degeneration. *Arch Ophthalmol*. 2004;122:598–614.
19. Wong RW, Richa DC, Hahn P, Green WR, Dunaief JL. Iron toxicity as a potential factor in AMD. *Retina*. 2007;27:997–1003.
20. Stocker R, Yamamoto Y, McDonagh AF, Glazer AN, Ames BN. Bilirubin is an antioxidant of possible physiological importance. *Science*. 1987;235:1043–1046.
21. Schipper HM, Song W, Zukor H, Hascalovici JR, Zeligman D. Heme oxygenase-1 and neurodegeneration: expanding frontiers of engagement. *J Neurochem*. 2009;110:469–485.
22. Nakagami T, Toyomura K, Kinoshita T, Morisawa S. A beneficial role of bile pigments as an endogenous tissue protector: anti-complement effects of biliverdin and conjugated bilirubin. *Biochim Biophys Acta*. 1993;1158:189–193.
23. Vogt SD, Curcio CA, Wang L, et al. Retinal pigment epithelial expression of complement regulator CD46 is altered early in the course of geographic atrophy. *Exp Eye Res*. 2011;93:413–423.
24. Rutar M, Natoli R, Kozulin P, Valter K, Gatenby P, Provis JM. Analysis of complement expression in light-induced retinal degeneration: synthesis and deposition of C3 by microglia/macrophages is associated with focal photoreceptor degeneration. *Invest Ophthalmol Vis Sci*. 2011;52:5347–5358.
25. Rohrer B, Guo Y, Kunchithapautham K, Gilkeson GS. Eliminating complement factor D reduces photoreceptor susceptibility to light-induced damage. *Invest Ophthalmol Vis Sci*. 2007;48:5282–5289.
26. Rouault TA, Hentze MW, Caughman SW, Harford JB, Klausner RD. Binding of a cytosolic protein to the iron-responsive element of human ferritin messenger RNA. *Science*. 1988;241:1207–1210.
27. Muckenthaler MU, Galy B, Hentze MW. Systemic iron homeostasis and the iron-responsive element/iron-regulatory protein (IRE/IRP) regulatory network. *Annu Rev Nutr*. 2008;28:197–213.
28. Carroll CB, Zeissler ML, Chadborn N, et al. Changes in iron-regulatory gene expression occur in human cell culture models of Parkinson's disease. *Neurochem Int*. 2011;59:73–80.
29. Kaur D, Lee D, Ragapolan S, Andersen JK. Glutathione depletion in immortalized midbrain-derived dopaminergic neurons results in increases in the labile iron pool: implications for Parkinson's disease. *Free Radic Biol Med*. 2009;46:593–598.
30. Wang L, Wang W, Zhao M, Ma L, Li M. Psychological stress induces dysregulation of iron metabolism in rat brain. *Neuroscience*. 2008;155:24–30.
31. Mueller S. Iron regulatory protein 1 as a sensor of reactive oxygen species. *Biofactors*. 2005;24:171–181.
32. Gnana-Prakasam JP, Thangaraju M, Liu K, et al. Absence of iron-regulatory protein Hfe results in hyperproliferation of retinal pigment epithelium: role of cystine/glutamate exchanger. *Biochem J*. 2009;424:243–252.
33. Harkewicz R, Du H, Tong Z, et al. Essential role of ELOVL4 protein in very long chain fatty acid synthesis and retinal function. *J Biol Chem*. 2012;287:11469–11480.
34. Chen Y, Okano K, Maeda T, et al. Mechanism of all-trans-retinal toxicity with implications for stargardt disease and age-related macular degeneration. *J Biol Chem*. 2012;287:5059–5069.